Design and construction of diverse mammalian prion strains

David W. Colby[a], Kurt Giles[a,b], Giuseppe Legname[a,b,1], Holger Wille[a,b], Ilia V. Baskakov[a,2], Stephen J. DeArmond[a,c], and Stanley B. Prusiner[a,b,3]

[a]Institute for Neurodegenerative Diseases and Departments of [b]Neurology and [c]Pathology, University of California, San Francisco, CA 94143

Contributed by Stanley B. Prusiner, September 11, 2009 (sent for review September 2, 2009)

Prions are infectious proteins that encipher biological information within their conformations; variations in these conformations dictate different prion strains. Toward elucidating the molecular language of prion protein (PrP) conformations, we produced an array of recombinant PrP amyloids with varying conformational stabilities. In mice, the most stable amyloids produced the most stable prion strains that exhibited the longest incubation times, whereas more labile amyloids generated less stable strains and shorter incubation times. The direct relationship between stability and incubation time of prion strains suggests that labile prions are more fit, in that they accumulate more rapidly and thus kill the host faster. Although incubation times can be changed by altering the PrP expression level, PrP sequence, prion dose, or route of inoculation, we report here the ability to modify the incubation time predictably in mice by modulating the prion conformation.

synthetic prions | stability | amyloid | neurodegeneration | conformation

For many years, investigators argued that the existence of prion strains demanded that an as yet undetected nucleic acid genome be buried within the infectious protein particles (1). Subsequent studies of prions in mammals and fungi, using prion proteins produced in mammals and bacteria as well as synthetic peptides, have demonstrated that prions are comprised solely of protein. In transgenic (Tg) mice overexpressing mouse prion protein (MoPrP) with a P→L substitution at position 101 corresponding to the mutation identified in humans who have Gerstmann-Sträussler-Scheinker disease, experimental Gerstmann-Sträussler-Scheinker was transmitted to Tg mice expressing low levels of MoPrP (P101L) (2–5). Similar transmissions were accomplished later with synthetic peptides consisting of 55 residues carrying the same P→L mutation that had been folded into a β-rich structure (6). A recombinant fragment of the Sup35NM protein was polymerized into amyloid fibrils and introduced into yeast (7). Similar studies were performed later for the Het-s and [URE3] fungal prions (8, 9). Subsequently, Sup35 NM protein fragments were used to produce different [PSI^+] strains, and these strains were introduced into yeast (10, 11). Concomitantly, a recombinant (rec) MoPrP fragment consisting of 140 amino acids was polymerized into amyloid and inoculated into Tg mice; the mice developed prion disease after prolonged incubation periods (12). These studies, and others (13) in mammals and fungi, have established beyond any reasonable doubt that prions are composed solely of protein.

In mammals, prions cause Creutzfeldt-Jakob disease (CJD) in humans, scrapie of sheep, bovine spongiform encephalopathy, and chronic wasting disease of deer (14–18). The disease-causing isoform of the mammalian prion protein (PrP^{Sc}) is an alternatively folded conformation of the normal, cellular prion protein. Naturally occurring prion strains have been isolated, each with a distinct incubation period and characteristic pathology; these traits often are conserved upon serial transmission (19, 20) and are not based on differences in the amino acid sequence of the protein. Biochemical evidence argues that each prion strain is enciphered by a distinct conformation of PrP^{Sc} (21–23).

In previous studies, synthetic prions were formed of recMoPrP during polymerization into amyloid fibers (12). Inoculation of PrP amyloid fibers into Tg9949 mice, which overexpress N-terminally truncated PrP at 16–32 times normal levels, led to the recovery of prions containing protease-resistant PrP^{Sc} and to neuropathological changes typical of prion disease. The conformational stability of the resulting prion isolate, as measured by the guanidine hydrochloride (GdnHCl) concentration required to denature half of the sample ($GdnHCl_{1/2}$) was unusually high (≈4.5 M), confirming the novelty of the prion strain generated (24). Subsequent serial passage of this isolate led to shortened incubation periods and a decrease in the conformational stability of the resulting prion isolate. Combining these data with those available for naturally occurring prion strains, we found that the conformational stability of prion isolates is directly proportional to the incubation period (25).

To gain insight into the conformational basis of prion strain diversity, we sought to create a spectrum of synthetic prion strains with different conformational stabilities. We hypothesized that it might be possible to produce prion strains with short, intermediate, and long incubation times by varying the conformational stability of the amyloid inoculum [supporting information (SI) Fig. S1]. To test this proposal, we created amyloid fibers under an array of conditions that resulted in the refolding of recMoPrP into distinct conformations. We postulated that the newly created synthetic prion strains would have conformational stabilities and incubation periods dictated by the properties of the amyloid preparations from which they were generated.

Results

To generate PrP amyloids with different conformational stabilities, we systematically altered the conditions used for their formation, including urea concentration, pH, and temperature (Fig. S2). The temperature of amyloid formation is an important determinant of yeast prion stability (10). We monitored the formation of amyloid using the fluorescent dye thioflavin T (ThT) (26). Decreasing the urea concentration (Amyloid 7) and temperature (Amyloid 8) resulted in amyloid fibers with lower conformational stability (Fig. 1). We also found that fibers formed of recombinant PrP (recPrP) (89–230) (Amyloid 6) had a lower conformational stability than those formed of recPrP(23–230) (Amyloid 5) under identical conditions (Fig. 1).

From the 11 amyloid preparations generated (Table S1), a subset with distinct conformational stabilities (Amyloids 5–8; Table 1 and Fig. 1) was selected for further characterization throughout this work. $GdnHCl_{1/2}$ values for different preparations ranged from 2.0

Author contributions: D.W.C., G.L., and S.B.P. designed research; D.W.C., K.G., H.W., I.V.B., and S.J.D. performed research; D.W.C., K.G., H.W., S.J.D., and S.B.P. analyzed data; and D.W.C., S.J.D., and S.B.P. wrote the paper.

The authors declare no conflict of interest.

[1]Present address: Neurobiology Sector, Scuola Internazionale Superiore di Studi Avanzati, Trieste 34151, Italy.

[2]Present address: Medical Biotechnology Center, University of Maryland Biotechnology Institute, Baltimore, MD 21201.

[3]To whom correspondence should be addressed. E-mail: stanley@ind.ucsf.edu.

This article contains supporting information online at www.pnas.org/cgi/content/full/0910350106/DCSupplemental.

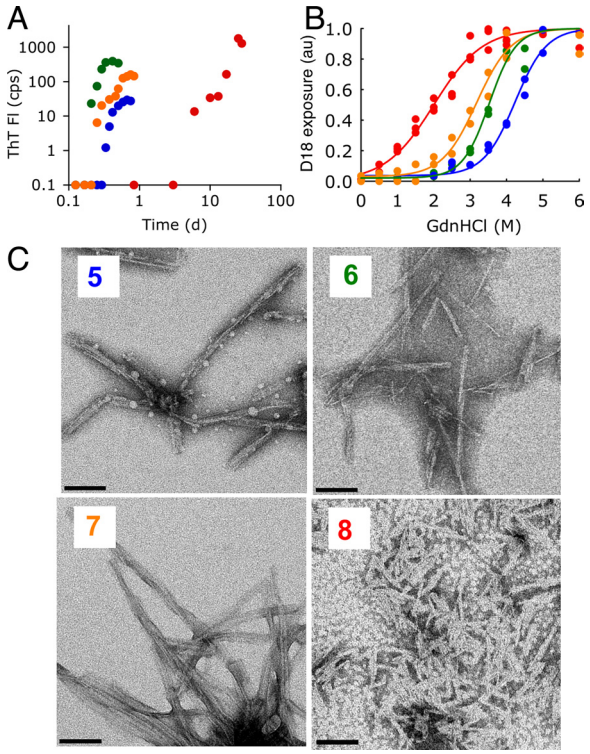

Fig. 1. Characterization of diverse PrP amyloid conformations. Formation of Amyloid 5 (*blue*), Amyloid 6 (*green*), Amyloid 7 (*orange*), and Amyloid 8 (*red*) was monitored by ThT fluorescence (*A*), followed by measurement of conformational stability by ELISA coupled with denaturation with increasing concentrations of GdnHCl (*B*). Electron micrographs (*C*) show morphology of Amyloids 5–8, as indicated. (Scale bars, 100 nm.)

M to 4.2 M (Fig. 1*B*), and distinct morphologies could be identified by electron microscopy (Fig. 1*C*). The fibers were sensitive to protease digestion under standard conditions used for detecting PrP^{Sc} in brain homogenates (20 μg/mL PK, 37 °C, 1 h) (Fig. S3*A*). Because of the unusual appearance of Amyloid 8, we verified that it was a true amyloid by testing its capability to seed amyloid formation (Fig. S3 *B* and *C*).

To determine infectivity, bioassays were performed in Tg4053 mice that overexpress full-length, wild-type MoPrP at 4–8 times normal levels and exhibit abbreviated incubation periods as compared with wild-type mice (27, 28). We also selected Tg4053 mice for these studies because we discovered that the Tg9949 mice used in previous studies develop late-onset neurological dysfunction that is distinct from and unrelated to prion disease, as do several lines of Tg mice overexpressing other PrPs (29); the occurrence of this unrelated neurological dysfunction complicates the determination of incubation periods in Tg9949 mice. When we monitored uninoculated Tg4053 mice as well as Tg4053 mice inoculated with BSA and PBS over their entire lifespans, we found that these mice were no more likely than wild-type FVB mice to develop spontaneous neurological dysfunction as they age ($P > 0.30$, Fig. S4). Neither Tg9949 nor Tg4053 mice spontaneously generate prions based on neuropathological examination, Western immunoblotting, activity in the amyloid seeding assay (ASA) (30), and serial transmission of brain homogenates (Fig. S4 and Table S2).

Table 1. Conditions used for formation of diverse amyloid fiber preparations[a]

Amyloid preparation	recMoPrP sequence	Urea (M)	Buffer, pH	NaCl (M)	Temperature (°C)
5	23–230	4	Acetate, pH 5	0.4	37
6	89–230	4	Acetate, pH 5	0.4	37
7	89–230	0.2	Acetate, pH 5	0.2	37
8	89–230	0.2	Citrate, pH 6	0.2	4

[a]A complete list of amyloid preparations generated for these studies can be found in Table S1.

We inoculated the 11 amyloid preparations, as well as monomeric recMoPrP as a negative control, into groups of 8–12 Tg4053 mice (Fig. 2 and Fig. S5). Of the 11 amyloid inocula, 10 caused disease in Tg4053 mice with incubation times greater than 475 days (Table S3). Mice inoculated with Amyloids 5, 6, and 7 developed prion disease (Fig. 2*A*), and their brains harbored PrP^{Sc} (Fig. 2*B*) of varying protease resistance (Table S4); we designated the resulting prion isolates "MoSP5," "MoSP6," and "MoSP7," respectively. Tg4053 mice inoculated with either Amyloid 8 or monomeric recPrP did not develop prion disease (Fig. 2*A*). We measured the conformational stability of protease-resistant PrP^{Sc} in the brains of mice harboring MoSP5, MoSP6, and MoSP7 (Fig. 2*C*) and found that the conformational stability for each isolate followed an order similar to that of the amyloid fibers used to create them. Analysis of the pooled results indicated that inoculation of Tg4053 mice with 30 μg of amyloid fibers significantly enhanced the probability of neurological dysfunction as compared with control groups ($P = 0.002$) (Fig. S5*A*).

Neuropathological analysis showed that the initial passage of Amyloids 5, 6, and 7 in Tg4053 mice caused prion disease. All 3 amyloid preparations resulted in the formation of punctate PrP^{Sc} deposits (1–4 μm) within the gray matter neuropil and adjacent to nerve cell bodies (Fig. 2*D*, *Top*). With all 3 prion amyloid preparations, varying degrees of vacuolation also were found in the neuropil (Fig. 2*D*, *Bottom*).

We serially transmitted brain homogenates containing 6 of the 10 new synthetic prion strains to Tg4053 mice (Fig. 3 and Table S5). After brains from ill Tg4053 mice were subjected to Western blotting following limited PK digestion, we inferred that isolates MoSP5, MoSP6, and MoSP7 with the greatest extent of protease resistance were likely to be the most mature forms and selected those isolates for further study (Table S4). Brain homogenates containing MoSP5, MoSP6, and MoSP7 transmitted disease to healthy Tg4053 mice (Fig. 3*A* and Table S5); MoSP6 and MoSP7 also transmitted disease to wild-type FVB mice (Fig. 3*B* and Table S5). We determined $GdnHCl_{1/2}$ values of MoSP5, MoSP6, and MoSP7 passaged in Tg4053 mice (Fig. 3*C*) and of MoSP6 and MoSP7 in FVB mice (Fig. 3*D*).

Distributions of neuropathological lesions as well as PrP deposits in the brain were unique for MoSP5, MoSP6, and MoSP7 (Fig. 4 and Fig. S6), suggesting that each is a unique strain. MoSP5, which resulted in the longest incubation time, caused a neuropathological phenotype characteristic of most scrapie prion isolates in rodents, including large numbers of vacuoles and finely granular PrP^{Sc} deposits in the gray matter neuropil. Amyloid plaques were not visualized by PrP immunohistochemistry or H&E staining, nor was substantial nerve cell loss detected. MoSP7, which resulted in the shortest incubation time during serial transmission in Tg4053 mice, produced many subcallosal amyloid plaques, which stained positive with thioflavin S, but less gray matter vacuolation than either MoSP5 or MoSP6. Additionally, the MoSP7 phenotype included severe loss of pyramidal cell neurons in the CA1 region of the hippocampus in 2 of 3 mice examined. Mice inoculated with MoSP6, which had an intermediate-duration incubation time, showed a mixed morphological phenotype: We observed moderately intense vacuolation, similar to that found with MoSP5, as well as numerous smaller, plaque-like deposits, suggesting amyloid deposition similar to that found with MoSP7. The plaque-like deposits measured 5–10 μm and localized to the subcallosal region and corpus callosum overlying the hippocampus. Neuropathology of MoSP6 and MoSP7 in FVB mice generally was consistent with that in Tg4053 mice. Vacuolation profiles revealed unique distri-

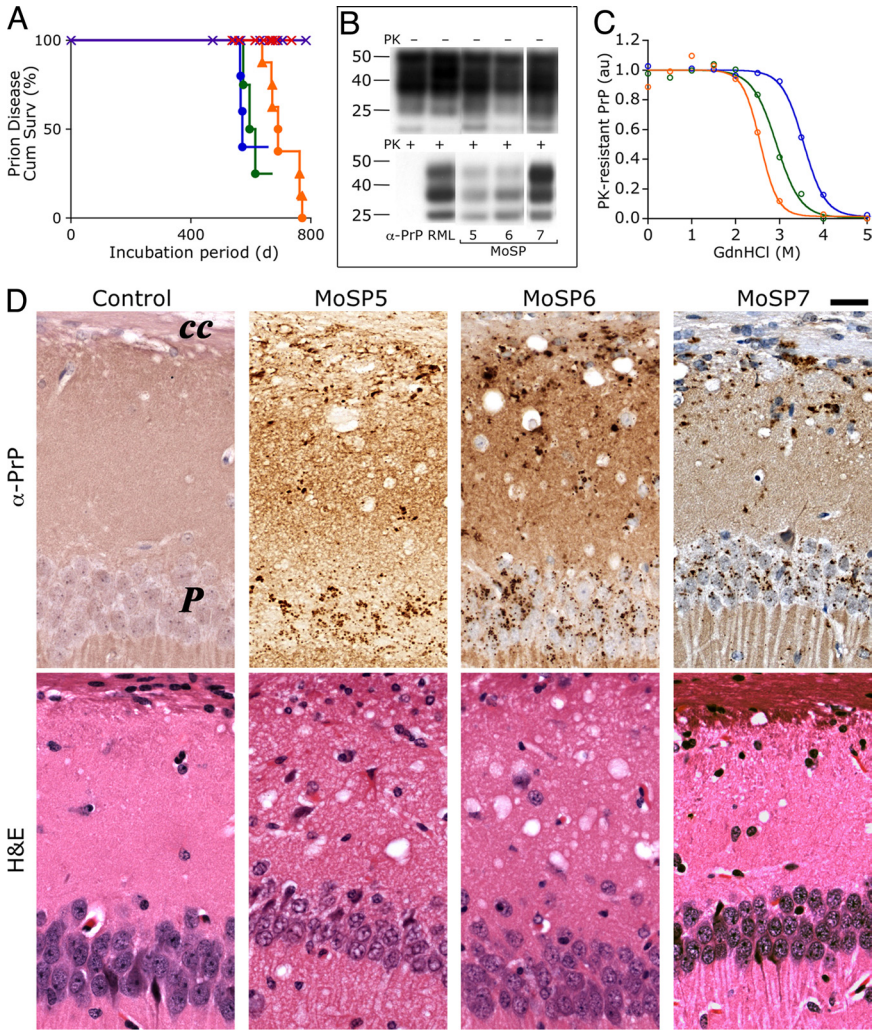

Fig. 2. Prion disease results from inoculation of Amyloids 5, 6, and 7 into Tg4053 mice. Amyloids 5 (*blue*), 6 (*green*), 7 (*orange*), and 8 (*red*) were inoculated into Tg4053 mice (n = 8–12 per inoculum). Monomeric, α-helical recPrP (*purple*) was inoculated as a control. Amyloids 5, 6, and 7 resulted in prion disease (*A*), which was confirmed by Western blotting for protease-resistant PrP^{Sc} (*B*) and neuropathology (*D*). The resulting isolates were designated ''MoSP5,'' ''MoSP6,'' and ''MoSP7,'' respectively. Amyloid 8 and monomeric recPrP did not result in prion disease; additional control experiments are shown in Fig. S4. The conformational stability of MoSP5 (*blue*), MoSP6 (*green*), and MoSP7 (*orange*) was measured by titration with GdnHCl followed by PK digestion (*C*). ●, mouse with symptomatic prion disease; ▲, mouse with asymptomatic prion disease; ×, deceased mouse with no indication of prions. In *B*, a mouse infected with RML prions is shown as a control for PK-resistant PrP^{Sc}. Molecular masses based on the migration of protein standards are shown in kDa. Neuropathology included PrP deposits (*dark brown*, *top row in D*) and vacuolation (*white holes*, *bottom row in D*). cc, corpus callosum; P, pyramidal cell layer. (Scale bar, 30 μm.)

butions of neuropathological lesions in the brains of Tg4053 mice serially infected with each new synthetic prion strain (Fig. S6). The well-defined differences in incubation times, neuropathology, and PrP immunohistochemical phenotypes that appeared during second passage of MoSP5, MoSP6, and MoSP7 in Tg4053 mice suggest that 3 distinct synthetic prion strains were formed.

We noted an apparent correlation of $GdnHCl_{1/2}$ values both with incubation periods and with the conformational stabilities of the amyloid fibers originally inoculated. To investigate these correlations further, we measured incubation periods and conformational stabilities of brain isolates from secondary serial passages of MoSP9, MoSP12, and MoSP13; these strains were created by amyloid fibers with conformational stabilities covering the same range of $GdnHCl_{1/2}$ values as those used to create MoSP5, MoSP6, and MoSP7 (Table S1). We found that the conformational stability of each synthetic prion strain was correlated closely to the conformational stability of the amyloid preparation used to generate it (Fig. 5*A*; $R = 0.94$, $n = 9$, $P = 0.0002$). Further, the conformational stability of the prion isolates correlated with the incubation period for the second passage, and the data appeared to separate into 2 distinct groups for Tg4053 and FVB mice (Fig. 5*B*; for Tg4053, $R = 0.993$, $n = 6$, $P < 0.0001$; for FVB, $R = 0.994$, $n = 3$, $P = 0.07$). The conformational stability of prion isolates from the first and second transmissions followed the same order observed for the amyloids used to generate them (Fig. 5*C*).

Discussion

In the foregoing studies, we generated an array of recMoPrP amyloid preparations with different conformational stabilities and showed that the resulting prion strains reflect the stabilities of the recMoPrP amyloids. Our data lead to 2 important conclusions: (*i*) The conformational stability of the synthetic prion isolate is dictated by the conformational stability of the recMoPrP amyloid from which it was generated, and (*ii*) Prions of higher conformational stability produce relatively longer incubation periods than those of lower stability. That we were able to generate different strains of prions that produce a range of incubation times in both wild-type FVB and Tg4053 mice by manipulating the conditions of recMoPrP

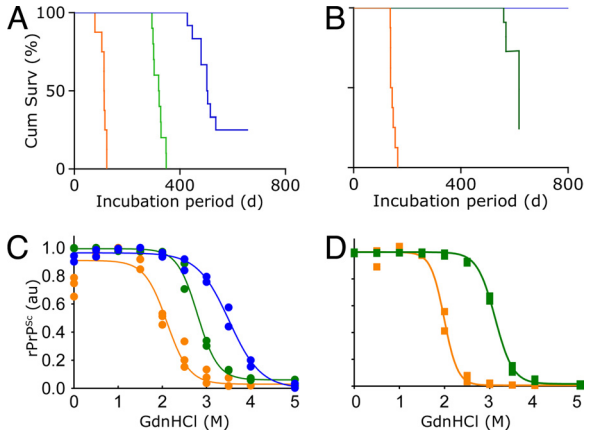

Fig. 3. New prion strains are serially transmissible and have distinct incubation periods and conformational stabilities. Serial transmission (*A*, *B*) and GdnHCl denaturation (*C*, *D*) of MoSP5 (*blue*), MoSP6 (*green*), and MoSP7 (*orange*) indicate 3 unique prion strains. (Primary data are shown in Fig. S7.) All 3 prion isolates were transmitted to Tg4053 mice (*A*, *C*); MoSP6 and MoSP7 were transmitted to wild-type FVB mice (*B*, *D*).

polymerization into amyloid is remarkable but was predicted by earlier studies (25, 31).

Amyloid 8, which had the lowest conformational stability, did not cause disease in Tg4053 mice. This particular amyloid may have been cleared readily by interstitial proteases because of its low stability. It also is possible that the animals did not live long enough for any of the putative prions in the sample to propagate and cause disease; however, this explanation runs counter to our data showing that low-stability prions exhibit short incubation periods. Finally, the conformation of PrP in Amyloid 8 simply may not encipher a prion state.

Our results establish beyond reasonable doubt that, like yeast prions (7, 9–11), mammalian prions are composed solely of protein and that infectivity resides within the polypeptide chain (12). Although many studies have implicated N-linked glycosylation of PrP as a site for specifying the properties of prion strains (17, 23, 32, 33), our findings militate against such proposals. Some of the apparent effects of N-linked glycosylation on the properties of prion strains may result from the changes in PrP turnover; diminished steady-state levels of mutant PrP occur with decreased glycosylation (32, 34). The recMoPrP used in the work described here was devoid of N-linked sugar chains as well as a glycosylinositol phospholipid anchor because *Escherichia coli* are known not to perform such posttranslational modifications. Mass spectrometry showed that the predicted and observed masses of the recMoPrPs agreed within <2 Da (35). This tight correspondence also eliminated other posttranslational chemical modifications such as phosphate, acetate, or sulfate groups as the basis of either prion infectivity or strain diversity in accord with earlier studies of PrP^{Sc} isolated from the brains of scrapie-infected hamsters (36).

Although our results confirm a relationship between the conformational stability of prions isolated from the brains of sick mice and disease incubation period as found previously (25), they also offer insight into the role of the PrP transgene and overexpression in this relationship. The correlation found in earlier work (reproduced as a dashed line in Fig. 5*B*) was based largely on measurements from Tg9949 mice, which overexpress PrP(89–230) at 16–32 times normal. We found that the slope of the correlation was more gradual for Tg4053 mice, which express full-length PrP at 4–8 times normal, and was slightly more gradual for wild-type FVB mice. This observation is consistent with the view that the conformational stability of a prion strain depends solely on its inherent conformation and is independent of the PrP expression level of the host animal. Indeed, for MoSP6, MoSP7, and MoSP12 passaged in both Tg4053 and FVB mice, the conformational stability was nearly identical regardless of the host.

Although our results ascertain that infection with lower-stability prions results in shorter incubation times and that infection with higher-stability prions results in longer incubation times, the mechanism remains to be determined. How the conformation of PrP^{Sc} determines the length of the incubation time is unknown. Although some prion strains with long incubation periods may be serially transmitted with high fidelity (1, 37), there is a propensity for prion strains to converge to shorter incubation times during repeated serial transmission. Generally, prion strains with shorter incubation times are favored because they replicate faster and kill the host before the strains with longer incubation periods can propagate. Nonetheless, examples of strain interference have been recorded in which a strain with a long incubation time interferes with the replication of a strain with a short incubation time (38, 39). Studies

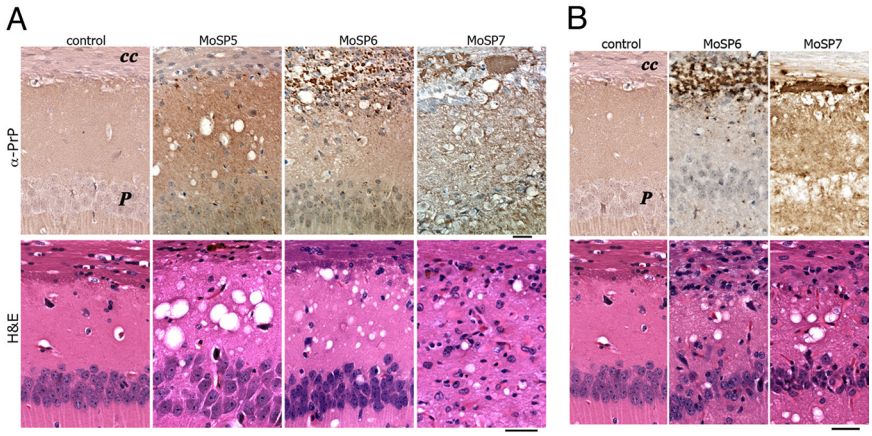

Fig. 4. Distinguishing neuropathology of MoSP5, MoSP6, and MoSP7. (*A*) PrP immunohistochemistry (*Top row*) shows finely granular PrP^{Sc} deposits in the hippocampal gray matter with MoSP5, coarsely granular, nonamyloid deposits of PrP^{Sc} primarily in the subcallosal-corpus callosum with MoSP6, and multiple, PrP-immunopositive amyloid plaques in the subcallosal region as well as abundant finely granular PrP^{Sc} deposits with MoSP7. H&E staining (*Bottom row*) shows large numbers of vacuoles with MoSP5, moderate numbers of vacuoles with MoSP6, and sparse numbers of vacuoles and severe nerve cell loss in the CA1 region with MoSP7. The control is a mock-inoculated Tg4053 mouse. (*B*) Neuropathology resulting from MoSP6 and MoSP7 initially transmitted in Tg4053 mice and then passaged to FVB mice shows a phenotype for MoSP6 and MoSP7 very similar to that found in Tg4053 mice. cc, corpus callosum; P, pyramidal cell layer. (Scale bars, 50 μm.)

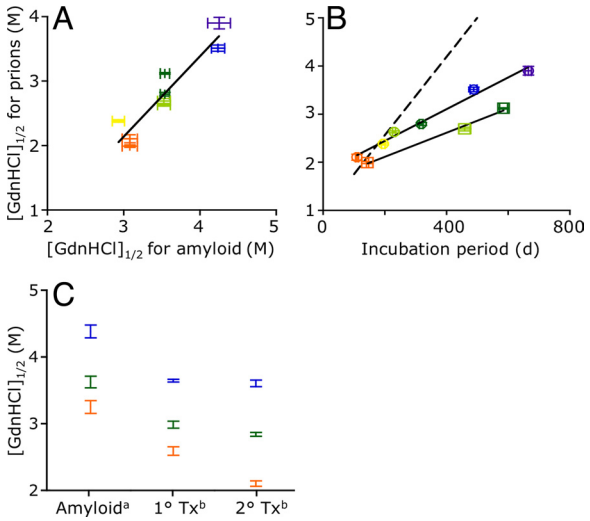

Fig. 5. The properties of new synthetic prion strains are modulated by the conformational stability of amyloids used to generate them. $GdnHCl_{1/2}$ values of synthetic prion strains directly correlated to the $GdnHCl_{1/2}$ values of the respective amyloid preparations (*A*: R = 0.94, $n = 9$, $P = 0.0002$), as well as to incubation periods (*B*: dashed line from ref. 25) in Tg4053 mice (○; R = 0.993, $n = 6$, $P < 0.0001$) and FVB mice (□; R = 0.994, $n = 3$, $P = 0.07$). MoSP5 (*blue*), MoSP6 (*green*), MoSP7 (*orange*), MoSP9 (*yellow*), MoSP12 (*lime*), MoSP13 (*purple*). Additional data for amyloids and prion isolates are shown in Tables S1, S3, and S5. Amyloids and synthetic prions retain their relative order of conformational stability during first (1° Tx) and second (2° Tx) transmission (*C*). [a]Amyloid conformational stability was measured by epitope exposure in ELISA; [b]MoSP conformational stability was measured by susceptibility to PK digestion.

of yeast have shown that many different chaperone proteins participate in the multiplication of fungal prions (40–42). Although investigations of mammalian prions have not yet identified specific auxiliary proteins that feature in replication (43, 44), recMoPrP may provide a tool for the identification of such replication-specific macromolecules.

Why did all the amyloid preparations have long incubation periods in the initial transmission (Fig. 2*A*)? A possible explanation is that a small number of infection-competent PrP^{Sc} conformers were formed among many noncompetent PrP molecules, resulting in very low titers in the inoculum. In that case, however, each amyloid preparation would have to contain a small subpopulation of infectious PrP^{Sc} molecules with conformational stabilities representative of the overall population. Instead, we found that the conformational stabilities of MoSP strains mimicked those of the bulk amyloid inocula. In light of this observation, a more likely explanation is that the PrP molecules in these amyloid preparations are intermediates, denoted "PrP*," along the folding pathway from cellular PrP to PrP^{Sc} (45). In this scenario, each amyloid preparation consisted of a distinct conformational intermediate (PrP*5, PrP*6, and PrP*7), which required maturation to generate MoSP5, MoSP6, and MoSP7 strains following inoculation. Another possibility could be that an inhibitor of prion replication was present in the amyloid preparations and required degradation before the disease could manifest. The second theory is consistent with the observed differences between the amyloid and the resulting prion strain, which included resistance to protease digestion and that brain deposits comprised of MoSP5 and MoSP6 did not bind thioflavin. The first and third explanations presented here would be consistent with our observations only if the infectious components of the amyloid preparations were present at low levels and eluded detection. It is imperative to obtain high-resolution structural data on the 3 amyloid preparations that gave rise to MoSP5, MoSP6, and MoSP7 and to establish a method to convert these intermediates into their fully infectious forms in vitro.

In earlier work, we observed that MoSP1 went through a gradual adaptation during repeated serial passage, with conformational stability and incubation period either decreasing or remaining constant from 1 passage to the next, depending on which brain isolate was passaged (24, 25). We expect that MoSP5, MoSP6, and MoSP7 will undergo a comparable adaptive process as we continue to passage these strains serially; indeed, the conformational stability of MoSP6 decreased during the second transmission (Fig. 5*C*), and preliminary findings on the third transmission support this hypothesis. Neither the mechanisms by which strains faithfully propagate nor the circumstances under which strains appear to adapt are well understood. What is clear is a tendency for adaptation to result in shorter, rather than longer, incubation periods through a Darwinian process in which the strain that kills the animal fastest nearly always dominates. A hypothesis for the apparent adaptation is that prion isolates actually are mixtures of strains with a distribution of incubation periods, and "strain adaptation" appears when a miniscule component with a short incubation period finally amplifies to sufficient titers to appear within the population. Alternately, strain adaptation may result from subtle conformational changes during or after prion replication. This hypothesis posits that only prion strains with high stability and a long incubation period are metastable and that prion molecules occasionally overcome an activation barrier to attain a lower-stability conformation. Although lower-stability conformations are not thermodynamically favored, such states could become populated via a kinetic trap (or "Brownian ratchet"), and the infrequency of crossing the activation barrier explains the stochastic occurrence of new metastable states. Ongoing serial-passage experiments of these novel synthetic prion strains may provide valuable insight into prion strain evolution.

The design of synthetic prions with specific properties seems likely to give new insights into the molecular pathogenesis of the more common neurodegenerative disorders, Alzheimer's disease and Parkinson disease (46–48). Understanding the age dependence and the mechanisms controlling the tempo of CJD may provide new strategies toward developing effective therapies for CJD as well as for Alzheimer's disease and Parkinson disease.

The incubation periods of prion disease have been shown to be influenced by many different factors: titers in the inoculum (49), the route of inoculation (50), and host PrP sequence (51) and expression levels (52). Here we demonstrate that incubation periods can be modulated directly by controlling the conformational stability of PrP. The identification of additional conformational properties of PrP that give rise to the biological properties of prion strains will give even greater insight into the molecular language through which PrP conformations encipher prion strains.

Methods

Detailed methods, including assays and biochemical, neuropathologic, and statistical analyses, are provided in *SI Methods*.

Fiber Formation. recMoPrP(89–230) and MoPrP(23–230) were expressed and purified as described (12, 53). Lyophilized protein was dissolved in 10 M urea at 10 mg/mL or in 5 M guanidine at 5 mg/mL, aliquoted, and frozen at −70 °C. To form fibers, solutions of urea (concentrations indicated in Table S1), 50 mM buffer (acetate, pH 4 and 5; citrate, pH 6; or Tris, pH 7 and 8), NaCl (concentrations indicated in Table S1), and 30 μM ThT were mixed before the addition of protein, which was added to a final concentration of 0.2 to 1.0 mg/mL. We added a 3-mm glass bead (Fisher Scientific) to each well of 96-microwell plates (Falcon 353945, BD Biosciences). Protein solution then was added (200 μL/well). Plates were shaken at the indicated temperature (Table S1) using either a microplate shaker placed in a refrigerator or an M2 fluorescence plate reader with automix capability (Molecular Devices), which also was used to obtain ThT fluorescence readings (filters set to 442 nm excitation, 485 nm emission). For reactions seeded with amyloid fibers, preformed fibers were added at 2% vol/vol. Fibers were dialyzed against PBS using 3 buffer changes to remove traces of urea and other solution components before further characterization.

Conformational Stability Measurements. To determine the conformational stability of amyloid fibers, a capture ELISA was used. The antibody D18 recognizes an epitope that is buried within the amyloid fibers but is exposed in soluble PrP; accessibility of this epitope was used to detect the fraction of PrP in amyloid versus soluble state. Fibers were dialyzed against PBS and then were added to GdnHCl (at the indicated final concentration), water, and BSA (final concentration 0.5%) and were mixed well. After 2-h incubation at room temperature, fiber solutions were mixed well and diluted 600-fold in PBS/BSA (0.1%) to reduce the GdnHCl concentration. To each well of a D18-coated, capture ELISA plate (54), 100 μL of denatured fiber solution was added, and the plate incubated overnight at 4° C. The plate was washed 3 times with Tris-buffered saline with Tween-20, and 100 μL of the antibody-enzyme conjugate P-HRP was added to each well. Following a 1-h incubation, the plate was washed 7 times with Tris-buffered saline with Tween-20 and was developed with 100 μL 2,2′-azino-bis(3-ethylbenzthiazoline-6-sulphonic acid (KPL, Inc). Absorbance was measured at 405 nm to determine soluble PrP in each well. A recPrP ladder was used to ensure that readings obtained were in the linear range. Fiber types were grouped based on their denaturation profiles (Fig. 1*B*; Table S1), given as approximate $GdnHCl_{1/2}$ values of 4.2 M, 3.5 M, 3.2 M, and 2.0 M.

The conformational stability of prion isolates was measured essentially as described (24), except that 50 μL of brain homogenate was mixed with 8 M GdnHCl and water to achieve the GdnHCl concentration indicated and a final volume of 133 μL. Following denaturation, GdnHCl concentrations were equalized by adding additional GdnHCl and/or water; these solutions were diluted in Tris buffer to dilute GdnHCl before PK digestion and Western blotting.

ACKNOWLEDGMENTS. We thank Christina G. Palmer, Hoang-Oanh B. Nguyen, Azucena Lemus, Ana Serban, Pierre Lessard, the staff at the Hunter's Point animal facility (University of California, San Francisco) for technical support, and Fred Cohen, David Glidden, and Jonathan Weissman (University of California, San Francisco) for discussions. This work was supported by gifts from the G. Harold and Leila Y. Mathers Foundation and the Sherman Fairchild Foundation, and by Grants NS064173, AG02132, AG10770, and AG021601 from the National Institutes of Health. D.W.C. was supported by the Jane Coffin Childs Memorial Fund for Medical Research and a National Institutes of Health Pathway to Independence Award.

1. Bruce ME, Dickinson AG (1987) Biological evidence that the scrapie agent has an independent genome. *J Gen Virol* 68:79–89.
2. Hsiao KK, et al. (1990) Spontaneous neurodegeneration in transgenic mice with mutant prion protein. *Science* 250:1587–1590.
3. Hsiao KK, et al. (1994) Serial transmission in rodents of neurodegeneration from transgenic mice expressing mutant prion protein. *Proc Natl Acad Sci USA* 91:9126–9130.
4. Tremblay P, et al. (2004) Mutant PrP^{Sc} conformers induced by a synthetic peptide and several prion strains. *J Virol* 78:2088–2099.
5. Nazor KE, et al. (2005) Immunodetection of disease-associated mutant PrP, which accelerates disease in GSS transgenic mice. *EMBO J* 24:2472–2480.
6. Kaneko K, et al. (2000) A synthetic peptide initiates Gerstmann-Sträussler-Scheinker (GSS) disease in transgenic mice. *J Mol Biol* 295:997–1007.
7. Sparrer HE, Santoso A, Szoka FC, Jr, Weissman JS (2000) Evidence for the prion hypothesis: Induction of the yeast [PSI^{+}] factor by in vitro-converted Sup35 protein. *Science* 289:595–599.
8. Maddelein ML, Dos Reis S, Duvezin-Caubet S, Coulary-Salin B, Saupe SJ (2002) Amyloid aggregates of the HET-s prion protein are infectious. *Proc Natl Acad Sci USA* 99:7402–7407.
9. Brachmann A, Baxa U, Wickner RB (2005) Prion generation in vitro: Amyloid of Ure2p is infectious. *EMBO J* 24:3082–3092.
10. Tanaka M, Chien P, Naber N, Cooke R, Weissman JS (2004) Conformational variations in an infectious protein determine prion strain differences. *Nature* 428:323–328.
11. King CY, Diaz-Avalos R (2004) Protein-only transmission of three yeast prion strains. *Nature* 428:319–323.
12. Legname G, et al. (2004) Synthetic mammalian prions. *Science* 305:673–676.
13. Jackson WS, et al. (2009) Spontaneous generation of prion infectivity in fatal familial insomnia knockin mice. *Neuron* 63:438–450.
14. Gajdusek DC (1977) Unconventional viruses and the origin and disappearance of kuru. *Science* 197:943–960.
15. Prusiner SB (1998) Prions. *Proc Natl Acad Sci USA* 95:13363–13383.
16. Caughey B, Baron GS (2006) Prions and their partners in crime. *Nature* 443:803–810.
17. Collinge J, Clarke AR (2007) A general model of prion strains and their pathogenicity. *Science* 318:930–936.
18. Aguzzi A, Sigurdson C, Heikenwaelder M (2008) Molecular mechanisms of prion pathogenesis. *Annual Review of Pathology* 3:11–40.
19. Dickinson AG, Meikle VM (1969) A comparison of some biological characteristics of the mouse-passaged scrapie agents, 22A and ME7. *Genet Res* 13:213–225.
20. Fraser H, Dickinson AG (1973) Scrapie in mice. Agent-strain differences in the distribution and intensity of grey matter vacuolation. *Journal of Comparative Pathology* 83:29–40.
21. Bessen RA, Marsh RF (1994) Distinct PrP properties suggest the molecular basis of strain variation in transmissible mink encephalopathy. *J Virol* 68:7859–7868.
22. Telling GC, et al. (1996) Evidence for the conformation of the pathologic isoform of the prion protein enciphering and propagating prion diversity. *Science* 274:2079–2082.
23. Collinge J, Sidle KCL, Meads J, Ironside J, Hill AF (1996) Molecular analysis of prion strain variation and the aetiology of ''new variant'' CJD. *Nature* 383:685–690.
24. Legname G, et al. (2005) Strain-specified characteristics of mouse synthetic prions. *Proc Natl Acad Sci USA* 102:2168–2173.
25. Legname G, et al. (2006) Continuum of prion protein structures enciphers a multitude of prion isolate-specified phenotypes. *Proc Natl Acad Sci USA* 103:19105–19110.
26. Rogers DR (1965) Screening for amyloid with the thioflavin-t fluorescent method. *Am J Clin Pathol* 44:59–61.
27. Carlson GA, et al. (1994) Prion isolate specified allotypic interactions between the cellular and scrapie prion proteins in congenic and transgenic mice. *Proc Natl Acad Sci USA* 91:5690–5694.
28. Telling GC, et al. (1996) Interactions between wild-type and mutant prion proteins modulate neurodegeneration in transgenic mice. *Genes Dev* 10:1736–1750.
29. Westaway D, et al. (1994) Degeneration of skeletal muscle, peripheral nerves, and the central nervous system in transgenic mice overexpressing wild-type prion proteins. *Cell* 76:117–129.
30. Colby DW, et al. (2007) Prion detection by an amyloid seeding assay. *Proc Natl Acad Sci USA* 104:20914–20919.
31. Tanaka M, Collins SR, Toyama BH, Weissman JS (2006) The physical basis of how prion conformations determine strain phenotypes. *Nature* 442:585–589.
32. DeArmond SJ, et al. (1997) Selective neuronal targeting in prion disease. *Neuron* 19:1337–1348.
33. Tuzi NL, et al. (2008) Host PrP glycosylation: A major factor determining the outcome of prion infection. *PLoS Biol* 6:e100.
34. Piro JR, et al. (2009) Prion protein glycosylation is not required for strain-specific neurotropism. *J Virol* 83:5321–5328.
35. Baskakov IV, Legname G, Baldwin MA, Prusiner SB, Cohen FE (2002) Pathway complexity of prion protein assembly into amyloid. *J Biol Chem* 277:21140–21148.
36. Stahl N, et al. (1992) Cataloguing post-translational modifications of the scrapie prion protein by mass spectrometry. *Prion Diseases of Humans and Animals*, eds Prusiner SB, Collinge J, Powell J, Anderton B (Ellis Horwood, London), pp 361–379.
37. Dickinson AG, Bruce ME, Outram GW, Kimberlin RH (1984) Scrapie strain differences: The implications of stability and mutation. *Proceedings of Workshop on Slow Transmissible Diseases*, ed Tateishi J (Japanese Ministry of Health and Welfare, Tokyo), pp 105–118.
38. Kimberlin RH, Walker CA (1985) Competition between strains of scrapie depends on the blocking agent being infectious. *Intervirology* 23:74–81.
39. Schutt CR, Bartz JC (2008) Prion interference with multiple prion isolates. *Prion* 2:61–63.
40. Chernoff YO, Lindquist SL, Ono B, Inge-Vechtomov SG, Liebman SW (1995) Role of the chaperone protein Hsp104 in propagation of the yeast prion-like factor [psi^{+}]. *Science* 268:880–884.
41. Shorter J, Lindquist S (2004) Hsp104 catalyzes formation and elimination of self-replicating Sup35 prion conformers. *Science* 304:1793–1797.
42. Chien P, Weissman JS, DePace AH (2004) Emerging principles of conformation-based prion inheritance. *Annu Rev Biochem* 73:617–656.
43. Telling GC, et al. (1995) Prion propagation in mice expressing human and chimeric PrP transgenes implicates the interaction of cellular PrP with another protein. *Cell* 83:79–90.
44. Perrier V, et al. (2002) Dominant-negative inhibition of prion replication in transgenic mice. *Proc Natl Acad Sci USA* 99:13079–13084.
45. Cohen FE, et al. (1994) Structural clues to prion replication. *Science* 264:530–531.
46. Meyer-Luehmann M, et al. (2006) Exogenous induction of cerebral beta-amyloidogenesis is governed by agent and host. *Science* 313:1781–1784.
47. Kordower JH, Chu Y, Hauser RA, Freeman TB, Olanow CW (2008) Lewy body-like pathology in long-term embryonic nigral transplants in Parkinson's disease. *Nat Med* 14:504–506.
48. Li JY, et al. (2008) Lewy bodies in grafted neurons in subjects with Parkinson's disease suggest host-to-graft disease propagation. *Nat Med* 14:501–503.
49. Prusiner SB, Cochran SP, Downey DE, Groth DF (1981) Determination of scrapie agent titer from incubation period measurements in hamsters. *Hamster Immune Responses in Infectious and Oncologic Diseases*, eds Streilein JW, Hart DA, Stein-Streilein J, Duncan WR, Billingham RE (Plenum Press, New York), pp 385–399.
50. Kimberlin RH, Walker CA (1978) Pathogenesis of mouse scrapie: Effect of route of inoculation on infectivity titres and dose-response curves. *J Comp Pathol* 88:39–47.
51. Westaway D, et al. (1987) Distinct prion proteins in short and long scrapie incubation period mice. *Cell* 51:651–662.
52. Tamgüney G, et al. (2006) Transmission of elk and deer prions to transgenic mice. *J Virol* 80:9104–9114.
53. Mehlhorn I, et al. (1996) High-level expression and characterization of a purified 142-residue polypeptide of the prion protein. *Biochemistry* 35:5528–5537.
54. Safar JG, et al. (2002) Measuring prions causing bovine spongiform encephalopathy or chronic wasting disease by immunoassays and transgenic mice. *Nat Biotechnol* 20:1147–1150.